

Diffraction production of $c\bar{c}$

Marta Łuszczak ², Rafał Maciuła ¹, Antoni Szczurek ^{1,2}

¹ Institute of Nuclear Physics PAN

PL-31-342 Cracow, Poland

² University of Rzeszów

PL-35-959 Rzeszów, Poland

At high-energies the gluon-gluon fusion is the dominant mechanism of $c\bar{c}$ production. This process was calculated in the NLO collinear as well as in the k_t -factorization approaches in the past. In this presentation we concentrate on production of $c\bar{c}$ pairs including several subleading mechanisms. This includes: $gg \rightarrow Q\bar{Q}$, $\gamma g \rightarrow Q\bar{Q}$, $g\gamma \rightarrow Q\bar{Q}$, $\gamma\gamma \rightarrow Q\bar{Q}$. In this context we use MRST-QED parton distributions which include photon as a parton in the proton as well as elastic photon distributions calculated in the equivalent photon approximation. We present distributions in the c quark (\bar{c} antiquark) rapidity and transverse momenta and compare them to the dominant gluon-gluon fusion contribution. We discuss also inclusive single and central diffractive processes using diffractive parton distribution found from the analysis of HERA diffractive data. As in the previous case we present distribution in c (\bar{c}) rapidity and transverse momentum. Next we present results for exclusive central diffractive mechanism discussed recently in the literature. We show corresponding differential distributions and compare them with corresponding distributions for single and central diffractive components. Finally we discuss production of two pairs of $c\bar{c}$ within a simple formalism of double-parton scattering (DPS). Surprisingly very large cross sections, comparable to single-parton scattering (SPS) contribution, are predicted for LHC energies.

1 Introduction

In this presentation we discuss contributions of some subleading mechanisms neglected in the analysis of $c\bar{c}$ production. We include contributions of photon-gluon (gluon-photon) as well as purely electromagnetic photon-photon fusion. Here we present only some selective results. The formalism and more details has been shown and discussed elsewhere¹.

We discuss also diffractive processes (single and central) in the framework of Ingelman-Schlein model corrected for absorption. Such a model was used in the estimation of several diffractive processes^{2,3,4,5}.

The absorption corrections are necessary to understand a huge Regge-factorization breaking observed in single and central production at Tevatron.

2 Production of heavy quarks

The cross section for the $c\bar{c}$ production, assuming gluon-gluon fusion, was calculated both in collinear and k_t factorization approaches. Our group has done detailed calculations in the second approach (see e.g. ^{6,7}).

In the leading-order (LO) approximation within the k_t -factorization approach the quadruply differential cross section in the rapidity of Q (y_1), in the rapidity of \bar{Q} (y_2) and in the transverse

momentum of Q ($p_{1,t}$) and Q ($p_{2,t}$) can be written as^{6,7}

$$\frac{d\sigma}{dy_1 dy_2 d^2 p_{1,t} d^2 p_{2,t}} = \sum_{i,j} \int \frac{d^2 \kappa_{1,t}}{\pi} \frac{d^2 \kappa_{2,t}}{\pi} \frac{1}{16\pi^2 (x_1 x_2 s)^2} \frac{1}{|\mathcal{M}_{ij \rightarrow Q\bar{Q}}|^2 \delta^2(\vec{\kappa}_{1,t} + \vec{\kappa}_{2,t} - \vec{p}_{1,t} - \vec{p}_{2,t})} \mathcal{F}_i(x_1, \kappa_{1,t}^2) \mathcal{F}_j(x_2, \kappa_{2,t}^2),$$

where $\mathcal{F}_i(x_1, \kappa_{1,t}^2)$ and $\mathcal{F}_j(x_2, \kappa_{2,t}^2)$ are the so-called unintegrated gluon (parton) distributions. The unintegrated parton distributions must be evaluated at:

$$\begin{aligned} x_1 &= \frac{m_{1,t}}{\sqrt{s}} \exp(y_1) + \frac{m_{2,t}}{\sqrt{s}} \exp(y_2), \\ x_2 &= \frac{m_{1,t}}{\sqrt{s}} \exp(-y_1) + \frac{m_{2,t}}{\sqrt{s}} \exp(-y_2), \end{aligned}$$

where $m_{i,t} = \sqrt{p_{i,t}^2 + m_Q^2}$.

3 Photon induced production of heavy quarks

The dominant contributions of heavy quark-antiquark production are initiated by gluon-gluon fusion or quark-antiquark annihilation. In general, even photon can be a constituent of the proton. This idea was considered by Martin, Roberts, Stirling and Thorne in Ref.⁹.

If the photon is a constituent of the nucleon then other mechanisms of $c\bar{c}$ production presented in Fig.1 are possible.

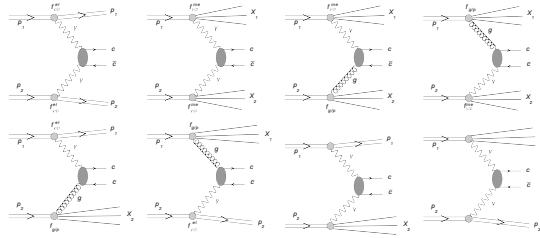


Figure 1: Diagrams representing photon-induced mechanisms of heavy quark production.

4 Results

4.1 Gluon-gluon fusion

Before we go to the new mechanisms we will present results for the dominant gluon-gluon fusion. In Fig.2 we show distributions in transverse momentum of c (or \bar{c}) for the gluon-gluon fusion mechanism for different popular choices of scales ($\mu^2 = 4m_c^2, M_{c\bar{c}}^2, p_t^2 + m_c^2$). We show our results for $\sqrt{s} = 500$ GeV (left panel) and $\sqrt{s} = 14$ TeV (right panel). In this calculation we have used GRV⁸ PDFs. The figure shows typical uncertainties due to the choice of the scale. We wish to stress here that at the higher energies the results of the calculations depend on the gluon distributions at small values of x .

4.2 γg and $g\gamma$ subprocesses

In Fig.3 we show transverse momentum distributions for the dominant gluon-gluon as well as for the subleading photon-gluon (gluon-photon) and photon-photon components for different

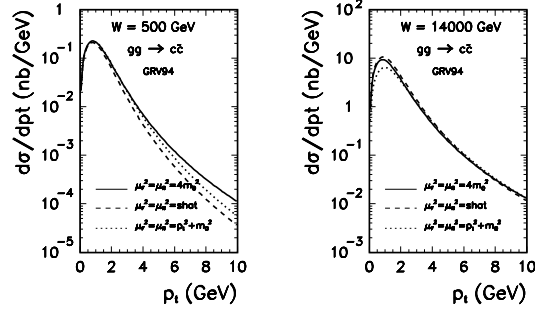


Figure 2: Distribution in quark/antiquark transverse momentum at $\sqrt{s} = 500$ GeV (left panel) and for $\sqrt{s} = 14$ TeV (right panel) for different choices of scales and for GRV gluon distribution.

gluon distribution functions^{8,9,10} for the RHIC energy $\sqrt{s} = 500$ GeV and for the nominal LHC energy $\sqrt{s} = 14$ TeV, respectively. At the LHC energy the results for different GPDs differ considerably which is a consequence of the poorly known small- x region. The differences at the energy $\sqrt{s} = 14$ TeV are particularly large which can be explained by the fact that a product of gluon distributions (both at small x) enters the cross section formula. New measurement of $c\bar{c}$ at the nominal LHC energy will be therefore a severe test of gluon distributions at small x and not too high factorization scales not tested so far. Similar uncertainties for the γg and $g\gamma$ are smaller as here only one gluon distribution appears in the corresponding cross section formula. The uncertainties for the photon distributions are not yet quantified.

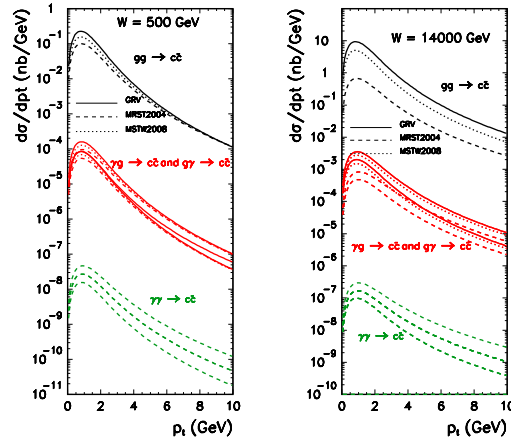


Figure 3: Transverse momentum distribution for the standard gluon-gluon mixed gluon-photon and photon-gluon as well as for photon-photon contributions for RHIC (left) and LHC (right).

It is very difficult to quantify uncertainties related to photon PDFs as only one set of PDFs includes photon as a parton of the proton. Here the isospin symmetry violation (not well known at present) would be an useful limitation. Our collection of the results for the photon induced mechanisms show that they are rather small and their identification would be rather difficult as the different distributions are very similar to those for the gluon-gluon fusion. Our intension is to document all the subleading terms. Our estimation shows that the sum of all the photon induced terms is less than 0.5 % and is by almost 2 orders of magnitude smaller than the uncertainties of the dominant leading-order gluon-gluon term.

5 Single and central diffraction

5.1 Formalism

The mechanisms of the diffractive production of heavy quarks ($c\bar{c}$) are shown in Figs.4, 5. The formalism how to calculate respective cross section has been presented elsewhere¹.

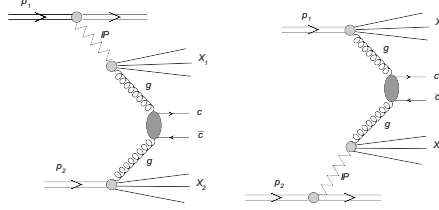


Figure 4: The mechanism of single-diffractive production of $c\bar{c}$.

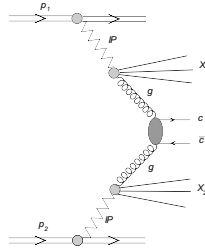


Figure 5: The mechanism of central-diffractive production of $c\bar{c}$.

5.2 Results

In Fig.6 we show transverse momentum distributions of charm quarks (or antiquarks). The distribution for single diffractive component is smaller than that for the inclusive gluon-gluon fusion by almost 2 orders of magnitude. Our results include gap survival factor¹. The cross section for central diffractive component is smaller by additional order of magnitude.

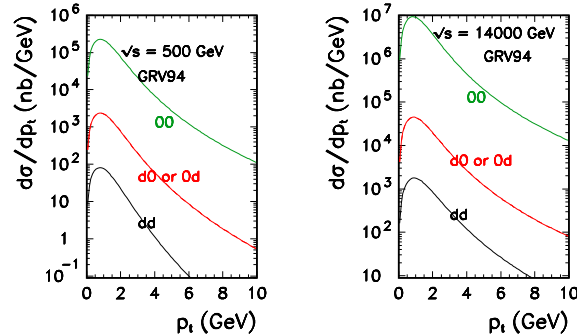


Figure 6: Transverse momentum distribution of c quarks (antiquarks) for RHIC energy $\sqrt{s} = 500$ GeV (left panel) and for LHC energy $\sqrt{s} = 14$ TeV (right panel) for the GRV94 gluon distributions. The result for single diffractive (0d or d0), central diffractive (dd) mechanisms are compared with that for the standard gluon-gluon fusion (00).

In Fig.7 we show distributions in quark (antiquark) rapidity. We show separately contributions of two different single-diffractive components (which give the same distributions in

transverse momentum) and the contribution of central-diffractive component in Fig.6. When added together the single-diffractive components produce a distribution in rapidity similar in shape to that for the standard inclusive case.

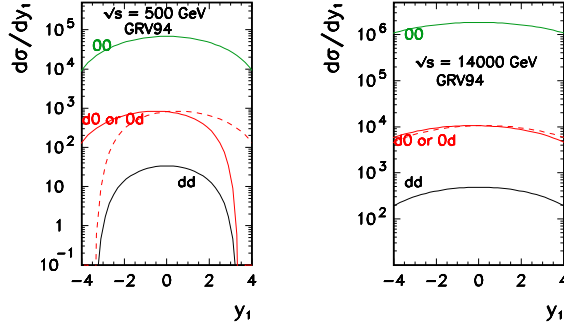


Figure 7: Rapidity distribution of c quarks (antiquarks) for RHIC energy $\sqrt{s} = 500$ GeV (left panel) and for LHC energy $\sqrt{s} = 14$ TeV (right panel) for the GRV94 gluon distributions. The result for single diffractive (0d or d0), central diffractive (dd) mechanisms are compared with that for the standard gluon-gluon fusion (00).

The cross section for single and central diffraction is rather small compared to the dominant gluon-gluon fusion component. However, a very specific final state should allow its identification by imposing special conditions on the one-side (single-diffractive process) and both-side (central diffractive process) rapidity gaps. We hope that such an analysis is possible at LHC. Special care should be devoted to the observation of the exclusive $c\bar{c}$ production. Without a special analysis of the final state multiplicity the exclusive $c\bar{c}$ production may look like an inclusive central diffraction.

6 Production of two $c\bar{c}$ pairs in double-parton scattering

The general formula for the cross section in terms of double-parton distributions can be written [11]:

$$d\sigma^{DPS} = \frac{1}{2\sigma_{eff}} F_{gg}(x_1, x_2, \mu_1^2, \mu_2^2) F_{gg}(x'_1, x'_2, \mu_1^2, \mu_2^2) d\sigma_{gg \rightarrow c\bar{c}}(x_1, x'_1, \mu_1^2) d\sigma_{gg \rightarrow c\bar{c}}(x_2, x'_2, \mu_2^2) dx_1 dx_2 dx'_1 dx'_2. \quad (1)$$

In Fig. 8 we compare cross sections for the single and double-parton scattering as a function of proton-proton center-of-mass energy. At low energies the conventional single-parton scattering dominates. At low energy the $c\bar{c}$ or $c\bar{c}c\bar{c}$ cross sections are much smaller than the total cross section. At higher energies the contributions dangerously approach the expected total cross section^a. This shows that inclusion of unitarity effect and/or saturation of parton distributions may be necessary. The effect of saturation in $c\bar{c}$ production has been included but not checked versus experimental data. Presence of double-parton scattering changes the situation. At LHC energies the cross section for both terms become comparable^b. This is a completely new situation when the double-parton scattering gives a huge contribution to inclusive charm production.

In Fig. 9, we present single c (\bar{c}) distributions. Within approximations made in this paper the distributions are identical in shape to single-parton scattering distributions. This means that double-scattering contribution produces naturally an extra center-of-mass energy dependent K

^aNew experiments at LHC will provide new input for parametrizations of the total cross section.

^bIf inclusive cross section for c or \bar{c} was shown the cross section should be multiplied by a factor of two – two c or two \bar{c} in each event.

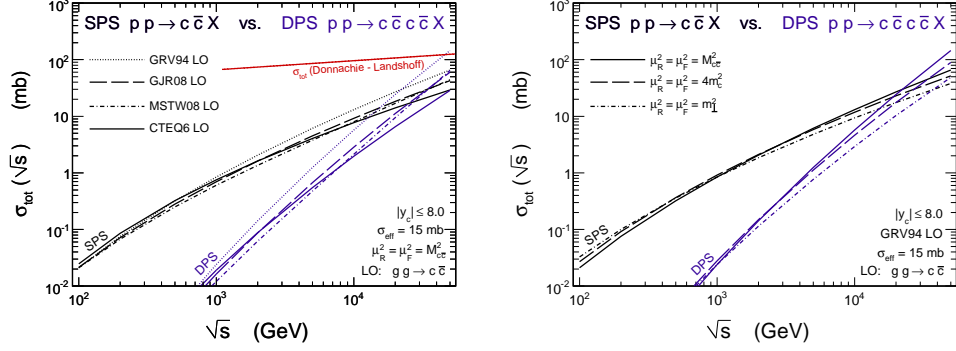


Figure 8: Total LO cross section for single-parton and double-parton scattering as a function of center-of-mass energy (left panel) and uncertainties due to the choice of (factorization, renormalization) scales (right panel). We show in addition a parametrization of the total cross section in the left panel.

factor to be contrasted with approximately energy-independent K -factor due to next-to-leading order corrections. One can see a strong dependence on the factorization and renormalization scales which produces almost order-of-magnitude uncertainties and precludes a more precise estimation. A better estimate could be done when LHC charm data are published and the theoretical distributions are somewhat adjusted to experimental data.

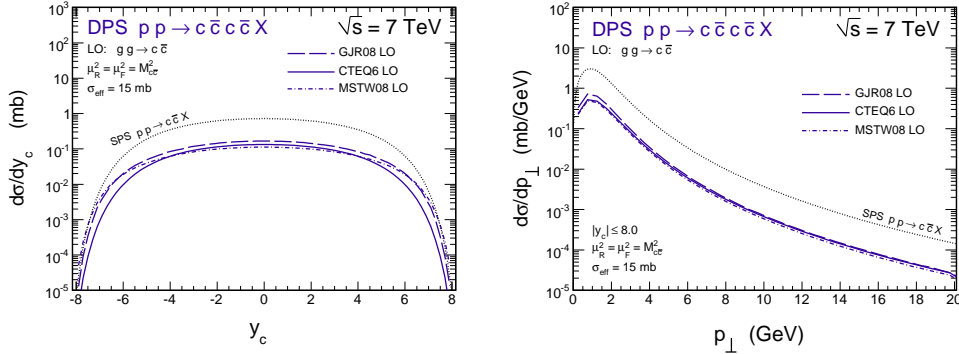


Figure 9: Distribution in rapidity (left panel) and transverse momentum (right panel) of c or \bar{c} quarks at $\sqrt{s} = 7$ TeV.

1. M. Łuszczak, R. Maciula and A. Szczurek, Phys. Rev. **D84** (2011) 114018.
2. G. Ingelman, P.E. Schlein, Phys.Lett.**B152** (1985) 256.
3. A. Berera, J.C. Collins, Nucl. Phys. **B474** (1996) 183;
R.J.M. Covelan and M.S. Soares, Phys. Rev. **D67** (2003) 077504.
4. M.V.T. Machado, Phys. Rev. **D76** (2007) 054006.
5. A. Aktas *et al.* [H1 Collaboration], Eur. Phys. J. C **48** (2006) 715.
6. M. Łuszczak and A. Szczurek, Phys. Rev. **D73** (2006) 054028.
7. M. Łuszczak, R. Maciula, A. Szczurek, Phys. Rev. **D79** (2009) 034009.
8. M. Gluck, E. Reya, A. Vogt, Eur.Phys.J. **C5** (1998) 461.
9. A.D. Martin, R.G. Roberts, W.J. Stirling, R.S. Thorne, Eur.Phys.J.**C39** (2005) 155.
10. A.D. Martin, W.J. Stirling, R.S. Thorne, G. Watt, Eur.Phys.J.**C39** (2009) 189.
11. M. Łuszczak, R. Maciula and A. Szczurek, hep-ph: 1111.3255.